Nonequilibrium simulation method for the study of directed thermal processing

D. K. Chokappa, S. J. Cook, and P. Clancy*

School of Chemical Engineering, Cornell University, Ithaca, New York 14853

(Received 7 November 1988)

A nonequilibrium molecular-dynamics computer-simulation method is developed for the study of directed thermal processing, in particular laser annealing. A strong heat gradient is applied to a substrate using entities called "energy carriers," which supply a given energy fluence over a given pulse duration with a known intensity-time shape (Gaussian, here). The thermodynamic, kinetic, and structural properties of the substrate are calculated during the ensuing melting and resolidification. Properties such as the melt depth, interface temperature, and interface velocity are calculated as a function of time, allowing predictions of the extent of superheating and supercooling to be made. From these results, the interface response function (interface velocity versus temperature) can be constructed. This function shows an asymmetry of melting and freezing kinetics (the former being significantly faster), in accord with recent experimental results. The sensitivity of the method to the modeling of the energy carriers, the system size, and pulse duration is discussed. Results are presented for a system of Lennard-Jones atoms, with an exposed (100) fcc face, and shown to be in good qualitative agreement with experimental results for silicon.

I. INTRODUCTION

In this paper, a new molecular-dynamics simulation technique is described for systems subjected to intense rapid heating under conditions far from equilibrium. The rationale behind the development of such a simulation method is to understand the kinetics and thermodynamics of phase transformations in solids occurring during rapid melting and resolidification. Such a study is applicable to the behavior of materials irradiated with a pulsed laser or electron beam. In laser processing of materials, energy is transferred to the material, usually in picosecond or nanosecond pulses, causing extreme conditions of very high thermal gradients and heat flows. These conditions give rise to interesting physical phenomena which have a direct bearing on the resulting properties of the processed material.

When a solid is irradiated using a laser pulse, a large temperature gradient is set up causing the substrate to melt. The solid-liquid interface thus formed is driven further into the solid substrate, at rapid velocity, by this large thermal gradient. Soon after the cessation of the pulse, heat flow into the substrate causes rapid quenching of the melt, often cooling the melt to temperatures well below the equilibrium freezing point. This undercooling of the melt creates a driving force in the reverse direction, which in turn causes the refreezing interface to move rapidly towards the surface. The resultant phase, crystalline or amorphous, is determined by the relative kinetics of the heat flow, the melt front, and the atomic rearrangement at the solid-liquid interface. The ultra-high quenching rates make it possible to study new crystal-growth mechanisms and amorphous solid or glass formation kinetics, and to form new metastable phases. Indeed, this facility of rapid heating and cooling has given rise to a whole new field of materials science, namely, directed energy processing. Processing techniques, such as rapid solidification, are of growing technological importance for materials such as semiconductors, metals, insulators, and ceramics. These techniques are capable of producing new materials whose properties (mechanical, structural, electronic) are tailored to specific requirements of the materials industry.

The physical processes, described above, take place at such fast rates and over such short time scales that experimental studies of the mechanisms involved are extremely difficult, if not impossible. Key variables, such as the temperature and velocity of the transient solid-liquid interface, require the development of highly sophisticated probes, e.g., temperature and optical sensors, that have high resolution both temporally and spatially. Synchrotron measurements by Larson et al.[1] and direct thermocouple measurements by Campisano[2] attempted to measure the interface temperature directly during pulsed melting. Such experiments are extremely difficult to perform and uncertainties in the results prevent direct, reliable calculations of the undercooling–interface-velocity relationship. Since reliable subnanosecond thermometry does not currently exist, there is an incentive to predict properties such as the interface temperature from theoretical models of the process.

A theoretical representation of processing techniques such as laser annealing must address several important issues: (a) the interaction of radiation with the material, (b) the representation of thermodynamic properties at conditions far from equilibrium, and (c) an adequate description of the kinetics and dynamics of phase transformations, e.g., rapid solidification. The purpose of this paper is to present a new method of supplying a thermal gradient within a nonequilibrium molecular-dynamics (NEMD) simulation in order to accurately describe the interfacial phenomena in directed thermal processing methods. The method will focus on providing information most valued by materials scientists, especially the

so-called interface response function (interface velocity versus interface temperature), which we shall show can be predicted from the results of one simulation run given only the energy fluence and pulse duration of the "laser."

In this paper we study a simple hypothetical system of Lennard-Jones (LJ) particles. The reason for choosing the LJ system first and not a Stillinger-Weber (SW) model for, e.g., silicon, lies in the fact that if we compared the results of our new NEMD model for a SW model of silicon with experiment, it would be difficult to assign the origin of any observed differences either to deficiencies in the NEMD method or to those inherent in the potential-energy function itself. It has already been observed by others that there are certain inadquacies in the modeling of silicon by the SW potential. We are in the process of obtaining experimental results for the laser annealing of the inert-gas solids, for which the LJ potential should be reasonably accurate, especially if a simple estimate of multibody forces is included. Comparison of experiment and NEMD simulation for the interface response function of the inert gases will allow us to refine the simulation method before proceeding to the study of more interesting, but more complex, materials such as metals, alloys, and semiconductors.

Section II briefly discusses related theoretical investigations. This is followed (Sec. III) by the description of the nonequilibrium molecular-dynamics simulation technique that models the interaction of an energy beam with a solid and calculates kinetic, dynamic, and structural properties of the transient solid-liquid interface. Finally, Sec. IV describes results for a system of Lennard-Jones atoms, originally arranged as a solid substrate which undergoes ultrarapid heating and, subsequently, rapid cooling.

II. PREVIOUS THEORETICAL AND COMPUTER-SIMULATION STUDIES

Some of the earliest theoretical investigations of rapid solidification were performed by Levi and Mehrabian,[3] Flemings,[4,5] and others, and were reviewed recently by Clyne.[6,7] These studies showed the necessity for significant undercooling of the melt prior to nucleation in order to obtain extremely high solidification rates and hence a stable planar growth front. A considerable volume of theoretical work in this area has been concerned with the solution of heat and mass transport models, based largely on conventional macroscopic diffusion equations. The first reported work was due to Baeri et al.,[8] who modeled pulsed-laser annealing of implanted semiconductors. A standard heat equation including laser-light absorption was solved numerically to give the time evolution of temperature and melting as a function of the pulse energy density and its duration. More recently, Wood et al.[9-11] published a series of papers in which they described a comprehensive theory for pulsed-laser annealing. The theory, as applied to silicon and to doped materials,[10] gave excellent agreement between experimental and calculated dopant profiles. Nonequilibrium interface segregation coefficients were related to the interface velocity using simple expressions which were

reasonably successful in reproducing experimental data.[11] Later work[12] removed the restriction preventing phase changes from occurring at temperatures other than the equilibrium melting temperature, thus allowing undercooling and superheating to be considered. Although such theoretical investigations allow experimental results to be fitted to phenomenological models, they fail to provide any fundamental information at the atomic level. Providing such an understanding of the dynamics and the atomic-scale processes which govern the kinetics of rapid thermal processing is more appropriately obtained from computer-simulation methods based in statistical mechanics.

There have been relatively few applications of computer-simulation techniques to the study of ultrarapid melting and freezing, although a considerable volume of information exists on equilibrium and steady-state dynamics and on the structure of the solid-liquid interface for simple model potentials.[13-23] Landman et al.[24] were the first to use a nonequilibrium molecular-dynamics (NEMD) technique to study the evolution, kinetics, and dynamics of an initially nonequilibrium system of Lennard-Jones (LJ) atoms in a supercooled state. They also performed the first simulation of a laser annealing experiment.[24] Their simulation cell consisted of a slab of 1500 atoms on fcc lattice sites interacting with a static extension of the crystal at one end and with a free surface at the other end. At the free surface, a pulse with a triangular intensity versus time profile and carrying a very small total energy of 6.3×10^{-5} J/cm^2 was applied. The coupling of the energy to the lattice was simulated through a scaling of the velocities of the particles using a chosen absorption profile. A system of LJ atoms was used to model a binary mixture of 90% argon and 10% krypton.[25,26] No significant degree of undercooling was observed in the proximity of the crystallization front. As a result of the imposed heating and subsequent resolidification, a perfect crystal was produced with a random substitutional impurity distribution. A small amount of impurity segregation was found at the free surface.

The only other NEMD studies of rapid solidification have been performed for silicon,[27,28] due partly to its enormous technological importance and, partly, to the availability of a suitable intermolecular potential function, namely, the popular Stillinger-Weber potential.[29] Abraham and Broughton[27] performed simulations of the pulsed heating of (100) and (111) surfaces of silicon. The energy pulse was added to the system by instantaneously raising the kinetic energy of the top four layers of one side of the solid slab at time zero. They found that the (111) crystal−melt interface propagates through layer-by-layer growth, whereas the (100) interface grows in a roughened manner with several layers growing at the same time. Landman et al.[28] reported experimental observations of the crystal-melt interface of silicon and accompanying molecular-dynamics simulations again using the Stillinger-Weber potential. Instead of their earlier practice of adding the energy time-stepwise, it was added instantaneously through scaling of particle layers in the top half of the solid slab, creating a liquid layer. The whole system was equilibrated at a temperature below the

triple-point temperature of silicon and subsequently allowed to evolve towards equilibrium. Unlike the results in (Ref. 27), Landman et al. found that the equilibrium crystal (100)-melt interface exhibited facets established on (111) planes, in agreement with the experimental observations. Finally, in recent papers, Kluge et al.[30,31] presented molecular-dynamics studies of the melting and quenching of silicon using the Stillinger-Weber potential model.[30] A 23-ps laser pulse of 0.2 J/cm^2 was used and the energy was deposited homogeneously within the volume at a constant rate over the 23-ps time interval. The crystal was found to superheat before the lattice became unstable and melted, as was found for the melting of Lennard-Jones atoms.[32] Amorphous silicon was formed by quenching the melt at 3×10^{14} K s^{-1},[28] showing good agreement with experimental structure-factor data.

The only calculation of the interface response function existing in the literature was made for a steady-state MD simulation of the solidification of LJ atoms by Broughton et al.[21] In their work the temperature throughout the cell was constant, whereas in the work to be presented here, there will be a strong heat gradient throughout the cell, and we shall consider both melting and resolidification to the extent and in the sequence dictated by the physical response of the system to the energy input.

III. THE NONEQUILIBRIUM MD METHOD

A. The simulation cell

The simulation cell used for the nonequilibrium studies contains a heterogeneous system of a solid in contact with a vapor. The cell is a square prism of fixed volume whose length in the z direction is 4 times that of its width, as shown in Fig. 1. The initial configuration consists of N atoms (here N=1000,2744,4096) arranged for this study in the lower half of the cell volume, on sites appropriate to a perfect fcc lattice. The choice of system size will be discussed in more detail later. The upper half of the cell contains a few ($N_g = 10$–15) randomly positioned atoms representing the vapor phase. For a system containing 1000 Lennard-Jones (LJ) atoms in the solid phase, the cell dimensions measure about $8\sigma \times 8\sigma \times 32\sigma$, while for a system containing 4096 LJ atoms the cell dimensions would be $12.5\sigma \times 12.5\sigma \times 50\sigma$ (i.e., roughly 128 atoms per atomic plane). The system size chosen has to be sufficiently large to overcome the stabilizing effect on the cubic symmetry of the cell induced by the periodic boundary conditions. This will be particularly important if we are to have any hope of accurately predicting the undercooling of the solid-liquid interface.

The initial configuration is obtained as follows. In the first stage, the solid portion of the simulation cell is obtained from an NPT (fixed N, fixed pressure, and fixed temperature) molecular-dynamics simulation. The cell used for the NPT simulation is also a square prism, with the same width as the cell in the nonequilibrium simulation cell. The length of the cell in the z direction is twice its width. The NPT simulation is carried out at a temperature below the triple point. The runs reported here were
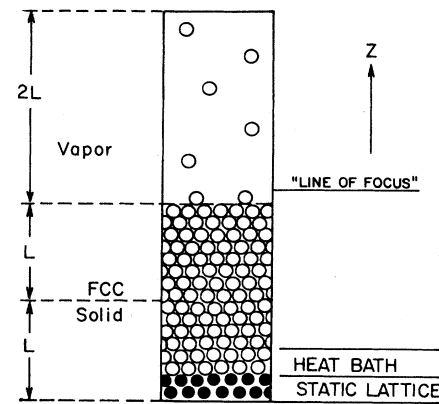
FIG. 1. Schematic diagram of the simulation cell used in modeling rapid solidification processes.

carried out for a system of LJ atoms initially at zero pressure and a reduced temperature of 0.4 ($\sim$60% of the equilibrium melting temperature). The NPT simulation is run for at least 50 000 time steps, with a reduced time step of 0.0046, i.e., for $\sim$500 ps, in order to equilibrate the system, as monitored via the pressure and energy of the system.

The final configuration from the NPT simulation is then read into a constant-temperature, constant-volume (NVT) simulation which creates a solid-vapor interface at one end and a fixed lattice at the other. The vapor phase has the same volume as the solid phase. This configuration is equilibrated for a further 50 000 time steps (with periodic boundary conditions in the lateral x and y directions only) in order to ensure that the interface is stable and immobile, as determined by observation of the singlet density profiles. The resulting configuration, shown in Fig. 1, is then used as the starting point for the NEMD studies.

In the NEMD runs, periodic boundary conditions are applied only in the two lateral directions (x and y) with a reflective wall at the top of the vapor section (i.e., in the positive z direction). The cell consists of four sections, as shown in Fig. 1. When N=4096 particles, the bottommost 400 atoms each time step are designated as a fixed lattice (i.e., roughly 3–4 planes of solid) whose atoms interact with the rest of the system but are held fixed in their initial positions. This acts like an external potential which stabilizes the system above it. The presence of a static lattice may introduce strain into the system, but it is expected that for sufficiently large systems this is unlikely to be a problem. Above the static lattice, the next 600 atoms are assigned as comprising the "heat bath." During the simulation, the velocities of the atoms in the heat bath are scaled (here every 20 time steps), using Brown and Clarke's method of thermostating,[33] in order to keep the temperature in the heat bath at a fixed value (taken to be the substrate temperature). The heat bath emulates the heat-conducting action of an underlying substrate, while the static lattice gives an impression of depth, in lieu of periodic boundary conditions in the z direction. Above the heat bath is the so-called dynamic section and, finally, the vapor section. It is within the dy-

namic section of the cell that all the interesting phenomena, relating to the kinetics of the transient solid-liquid interface, are expected to occur. The atoms in the dynamic section interact with the rest of the system through the interatomic forces and with the incoming energy "beam."

B. Coupling of the energy "beam" with the system

In this study, a laser or electron beam is considered merely a source of directed energy. It is assumed that the energy beam impinges uniformly on the surface and that all the affected atoms (both on the surface and within the substrate) are energized at the same instant of time. The only information we require of the energy beam is its power or energy, pulse duration, and the shape of the intensity-versus-time curve of the pulse. The potential models and the energy-transfer mechanism used in this study are not intended to represent the electronic properties of the material under study; hence the optical properties of the beam (i.e., wavelength and nature of beam) and of the irradiated material (absorption coefficient, etc.) cannot be modeled using this NEMD method. The reflectivity changes which result from the phase change (solid to liquid) of the material are incorporated into the simulation, as will be explained later in this section. It is assumed that the energy is transferred to the lattice system in the form of thermal or kinetic energy directly. At present, the model ignores the behavior of the real system during the first picosecond or so where the photons interact with the electronic states of the system to form a plasma, before the energy is converted to kinetic energy.

The shape of the intensity versus time pulse is assumed to be Gaussian, since this is the type commonly found experimentally. The pulse is characterized by a power, P (W/cm^2), or energy fluence, E (J/cm^2), and a pulse duration τ_P. The energy is supplied to the system every time step for the duration of the pulse (typically of the order of picoseconds to nanoseconds). The energy available to the system, ΔE, in one time step, Δt, at any time t during the action of the pulse, is obtained by integrating the Gaussian pulse from time to time $t + \Delta t$.

The crucial step of modeling the energy transfer to the system is effected through the interaction of the substrate atoms with so-called "energy carriers." The concept of an energy carrier was invoked to devise a mechanism for the energy transfer and not as a model for the energy beam itself. In this sense, these energy carriers are fictitious entities and should not have any physical characteristics other than the fact that they carry energy. At any time t during the action of the pulse, the available energy ΔE is distributed equally among N_c energy carriers in the form of kinetic energy only. The energy given to a single energy carrier is equipartitioned among all three translational degrees of freedom, giving no directional bias to the movement of the energy carriers. The speed of an individual energy carrier is obtained from a simple energy balance and is given in reduced units by

$$V^* = \left[\frac{2\Delta E^*}{N_c(m_c/m)} \right]^{1/2} , \tag{1}$$

where m_c is the mass of an energy carrier and m is the

mass of a system atom. Each energy carrier collides with a system atom, transfers its energy elastically, and disappears. As a result of the collision, the velocity of the system atom is changed. Using simple energy and momentum balances, the new velocity components of an atom in the system become

$$v_{2x}^* = \left[\frac{m_c}{m} \right] V_x^* + v_{1x}^* ,$$

$$v_{2y}^* = \left[\frac{m_c}{m} \right] V_y^* + v_{1y}^* , \tag{2}$$

$$v_{2z}^* = \left[\frac{m_c}{m} \right] V_z^* + v_{1z}^* ,$$

where

$$V_x^* = V_y^* = V_z^* = \frac{V^*}{\sqrt{3}} = \left[\frac{2\Delta E^*}{3N_c(m_c/m)} \right]^{1/2} . \tag{3}$$

In order to model the energy transfer in a more realistic way, the collisions are carried out only on atoms that are positioned below a certain z level (shown as the "line of focus" in Fig. 1) in the simulation cell. Here this level is chosen arbitrarily to be about one interplanar spacing above the original solid-vapor interface, but we are investigating how to relate the position of the line of focus to a known change in reflectivity of the substrate on melting, as will now be explained. As the solid is heated, it expands and eventually melts, causing some of the atoms to lie above the line of focus. This portion of the system is now unaffected by the energy carriers at the next time step. The first N_c atoms closest to the top face of the cell are selected for energy transfer, but collisions with the energy carriers are only carried out on $N_c - n$ atoms, where n is the number of atoms above the line of focus. This effectively changes the number of collisions every time step. The exclusion of these n atoms from the collision process serves several purposes. The first is concerned with emulating the focusing action of a laser. Second, if allowed, collisions of the energy carriers with the vapor particles would repeatedly energize them during the "irradiation," causing excessive vaporization. Third, and most important, such a collision procedure provides a way of changing the energy absorption characteristics of the system during the action of the pulse, albeit in a simple way. Although the total available energy per time-step, ΔE, is divided equally among N_c carriers, only $(N_c - n)(\Delta E/N_c)$ amount of energy is actually transferred to the system. This means that some of the energy, $n \Delta E/N_c$, is lost in the transfer process. This loss of energy may be seen as the change in absorption characteristics or reflectivity of the system with change in temperature and density. Thus, in a simple way, the change in reflectivity upon melting is built into the energy-transfer mechanism.

After the chosen energy has been supplied to the system for a specified pulse duration, the system is allowed to anneal long enough to achieve its final equilibrium configuration, as determined by the constancy of its thermodynamic and structural properties. Although no more

energy is added to the system, the annealing process is not at constant energy due to the presence of the heat bath, which slowly extracts energy from the system in order to restore the system to its original temperature. The final equilibrium configuration is reached when all the melt resolidifies and the temperature of the whole system returns to its original (i.e., preirradiation) value. This annealing process involves a simulation run time of roughly 10–50 times that of the pulse duration, depending on the fluence of the beam. A typical throughput of $\sim$4000 time steps per CPU hour on an IBM 3090-600E was achieved for the largest system through extensive vectorization of the code.

C. Property calculation during melting and solidification

The response of the material to the energy input supplied by the energy carriers is monitored through a study of the "local" thermodynamic, structural, and kinetic properties of the system at any given z distance measured from the bottom of the simulation cell. These properties are time dependent, and therefore the appropriate ensemble averages cannot be computed in the same way as those for equilibrium molecular-dynamics simulations. The oxymoronic term "local thermodynamics" bears some explanation. The system is divided into slices parallel to the original solid-vapor interface. Within each slice, smoothed values of the density, temperature, potential energy, radial distribution function, and mean-square displacement (MSD) are calculated using ensemble averages taken over a short time span. This procedure invokes Hoover's dictum[34] that "the local instantaneous properties should describe macroscopic behavior given that the constraints which we have placed on the system are physically realistic, or at least approach such a realism as the size of the system is increased."

For the singlet density function, $\rho(z)$, the thickness of each slice is such that 16 slices make one atomic layer. For the other properties, the thickness of each slice is such that it encloses one atomic layer. The single density is calculated as $n(z)/A \, \Delta z$, where $n(z)$ is the number of atoms in a layer centered at z, A is the cross-sectional area, and Δz is the thickness of the layer. The in-plane (2D) radial distribution function $g(r,L)$ is calculated for each layer according to

$$g(r,L) = \left\langle \left[\frac{A}{N_L} \right] \left[\frac{n(r,L)}{2\pi r \, \Delta r} \right] \right\rangle , \tag{4}$$

where N_L is the number of atoms in layer L, and $n(r,L)$ is the number of atoms in layer L between r and $r+\Delta r$. The MSD is calculated for each degree of freedom as

$$\langle X^2(t) \rangle = \left[\frac{1}{N_L} \right] \sum_{i=1}^{N_L} [X_i(t) - X_i(0)]^2 . \tag{5}$$

During rapid melting, when the properties within a layer change rapidly, the value of a property at any time t is taken as its time average over a very small number of time steps, here 50 times steps ($\sim$0.5 ps), being a compromise between obtaining acceptable statistical variability and capturing the rapid changes in the observable phenomena. During regrowth or annealing, when changes in the properties occur relatively slowly, the averages are taken over 100–500 time steps (1–5 ps).

As mentioned earlier, one of the primary goals of this study is to determine the structure and dynamics of the transient solid-liquid interface. The position and temperature of the interface at a given time are obtained from an analysis of the properties of the slices, especially the singlet density profile and the layerwise $g(r)$. However, uniquely determining the position of the interface is not an easy matter, especially for a diffuse interface such as that for the (100) fcc face of LJ atoms. Our procedure is as follows. We first determine the z position at which $g(r)$ exhibits completely liquidlike structure. For example, in Fig. 2, we show two-dimensional $g(r)$ functions at different locations in the cell after 45 ps. In this instance, it can be seen that the layer centered at a distance, $d=4.74\sigma$ from the original location of the solid-vapor interface still has largely crystalline structure, whereas the layer centered at $d=2.97$ has lost its solid structure. The layer at $d=3.86\sigma$ is judged to still have some solidlike structure. From this information, the location of the liquid side of the interfacial region at $t=30$ ps is taken to be 2.97σ away from the original solid-vapor interface, with an uncertainty of $\pm 0.45\sigma$. The two-dimensional density profile is then used to determine the z value corresponding to the loss of completely solidlike behavior (through the appearance of nonzero minima and taking into consideration the peak height). These two values, the loss of solidlike behavior and the onset of liquidlike structure, define the width and approximate location of the interfacial region.

Corroboration of this determination of the location and extent of the interfacial region was provided by an analysis of the atomic positions within the cell, postprocessing the configurations through a computer-graphics work station using specially written software.[41] Traversing from the bottom of the cell, we observed regular fcc
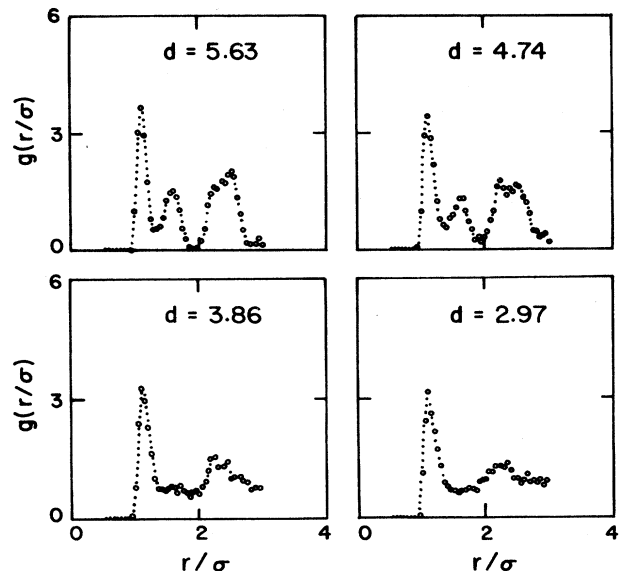
FIG. 2. In-plane radial distribution function $g(r)$ in units of the collision diameter σ at different depths d from the position of the original solid-vapor interface. Shown here are results at 45 ps for $d=5.63\sigma$, 4.74σ, 3.86σ, and 2.97σ.

crystalline planes of 128 atoms at a constant lattice separation up to a certain location, which was noted as the onset of the interfacial region. Above this z value the lattice separation was no longer the same. This is in agreement with Ref. 19, where the (100) fcc face was shown to melt such that it keeps the number of atoms constant but changes the lattice spacing in order to finally achieve the appropriate liquid density. Accordingly, we then analyzed the interfacial region by plotting the positions of 128 atoms at a time. Such an analysis shows a gradual change from a largely crystalline to a random orientation of atoms. The onset of completely liquidlike behavior was taken to be the end of the interfacial region. We were encouraged to observe that the results of the computer-graphics analysis were in reasonable agreement with those derived from $\rho(z)$ and $g(r)$. The results led us to associate an uncertainty in the position of the interface of $\pm 0.5\sigma$. It is worth noting that this is well within experimental uncertainty. The most difficult assignment of the interface location occurs at times corresponding to the maximum melt depth of the system, as will be discussed later.

The interface temperature can be estimated from the temperature-depth profiles once a value for the interface location has been found. Even during the rapid melt-in period, where experimental measurements are very difficult, the position and temperature of the interface can be determined the plotted as a function of time during both the melting and regrowth stages. The velocity of the interface at any time is estimated from the slope of a mean curve through the data points. The extent of superheating or supercooling can thus be predicted and related to the velocity of the interface. This feature of the simulation clearly demonstrates the advantage of this NEMD method over models based on continuum heat-transport equations. Profiles such as these can be obtained using this simulation method without either imposing any constraints, e.g., the melting transition occurring at the equilibrium melting point or specifying a certain amount of undercooling, as do many theories and other computer simulation methods.

IV. RESULTS FOR A LJ SYSTEM

The new NEMD method was tested for a material described by a simple potential-energy model in order to establish whether or not the model emulates the properties and dynamics of the transient solid-liquid interface in a realistic way and to determine important infrastructural details of the method, e.g., the minimum system size and suitable values for the simulation parameters, e.g., the mass and number of energy carriers. The test substance chosen for this task is described by a truncated Lennard-Jones (LJ) potential; the cutoff radius used here is 3σ. The mass of each substrate atom was chosen to be that of argon, and the potential parameters ε/k and σ are set to the values 119.8 K and 0.3405 nm, commonly used for a LJ model of argon. A time step of 10^{-14} s ($\Delta t^* = 0.0046$) was used to integrate the equations of motion using a modified "leap frog" algorithm.[18]

The original configuration of the system (as shown in Fig. 1) consisted of 1000–4096 LJ atoms located on (100)

fcc lattice sites, with a vapor phase containing 10–15 LJ atoms. The configuration was equilibrated at a reduced temperature, $T^* = kT/\varepsilon = 0.4$, or roughly 62% of the triple-point temperature of this system ($T_{tp} \sim 0.65$). At this temperature, the reduced density of the solid, $\rho\sigma^3$, is 1.0127 and the atoms in the solid phase pack into 20–32 atomic planes parallel to the solid-vapor interface. An energy pulse of 15 ps duration with an energy fluence of 25 mJ/cm^2 was chosen to "irradiate" the system. The optimum number of energy carriers was found to be $\sim N/2$ and the mass ratio m_c/m was taken to be 10^{-6}. A later section (IV B) will contain the sensitivity analysis of the results to m_c and N_c which led to the assignment of these values.

The result of "irradiating" and annealing the above system was analyzed in terms of the singlet density profiles $\rho(z)$, the in-plane radial distribution function $g(r)$, and using computer-graphics–derived snapshots of the atomic configurations as described in Sec. III C. Figure 3 shows the density profiles obtained at various times during the application of the pulse and during the annealing process. It can be seen from this figure that shortly after the conclusion of the pulse about one-fourth of the solid had melted. Following cessation of energy input, the solid continues to melt for a short time before recrystallization starts. The recrystallization occurs in a roughened manner (i.e., over several planes at a time), as found for the steady-state moving interface of a LJ system.[16] Figure 4 shows representative temperature profiles throughout the simulation cell at various times. It can be seen that the system took over 160 ps to fully recrystallize and for the temperature in the whole system to return to its original value. The annealing time required is thus over 10 times the duration of the pulse.

The position of the solid-vapor interface during processing was found to have changed, having expanded about 3.5σ in the space previously occupied by the vapor. An analysis of the structure of this final layer was made from both $\rho(z)$ and $g(r)$, and by postprocessing the atomic configurations of the uppermost layers of atoms using computer-graphics techniques. These showed that the regrowth had resulted in planes of atoms occupying fcc lattice sites with few defects, except for the final layer. This uppermost layer was clearly noncrystalline, with the appearance of a three-dimensional clustering of atoms, resembling a pool on the surface. The structure of this final layer could be the result of adsorption or of wetting. If, as the pressure is increased, the layer grows according to a power law, diverging at the saturation pressure, it will be a true wetting layer. It somewhat resembles a Volmer-Weber adsorption growth.[35] The genesis and time history of this clustering is now under investigation.

The properties of the slices were analyzed as described in Sec. III C, in order to determine the location of the interfacial region. The melt depth at time t is assigned to be the distance from the original solid-vapor interface to the (new) position of the midpoint of the solid-liquid interfacial at time t, as shown in Fig. 5. For qualitative comparison, an experimentally determined curve of the melt depth versus time for silicon[36] is also shown in Fig. 5. The simulation-derived data can be seen to exhibit all
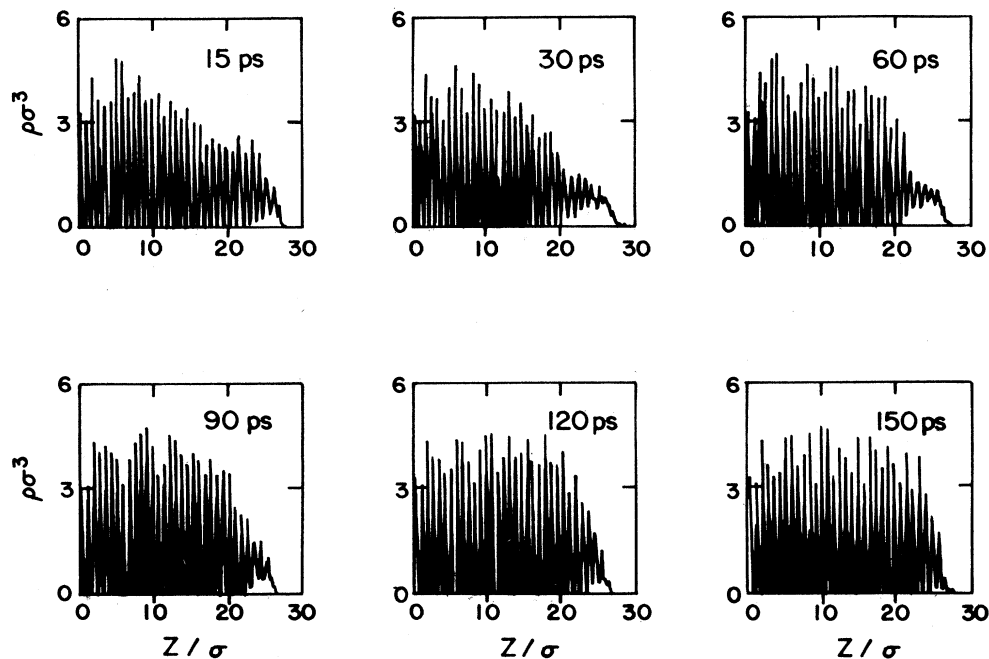
FIG. 3. Density profiles $\rho\sigma^3$ as a function of position in the simulation cell, z/σ. $Z = 0$ corresponds to the bottom of the cell. Results are shown at 15- and at 30-ps intervals from 30 to 150 ps.
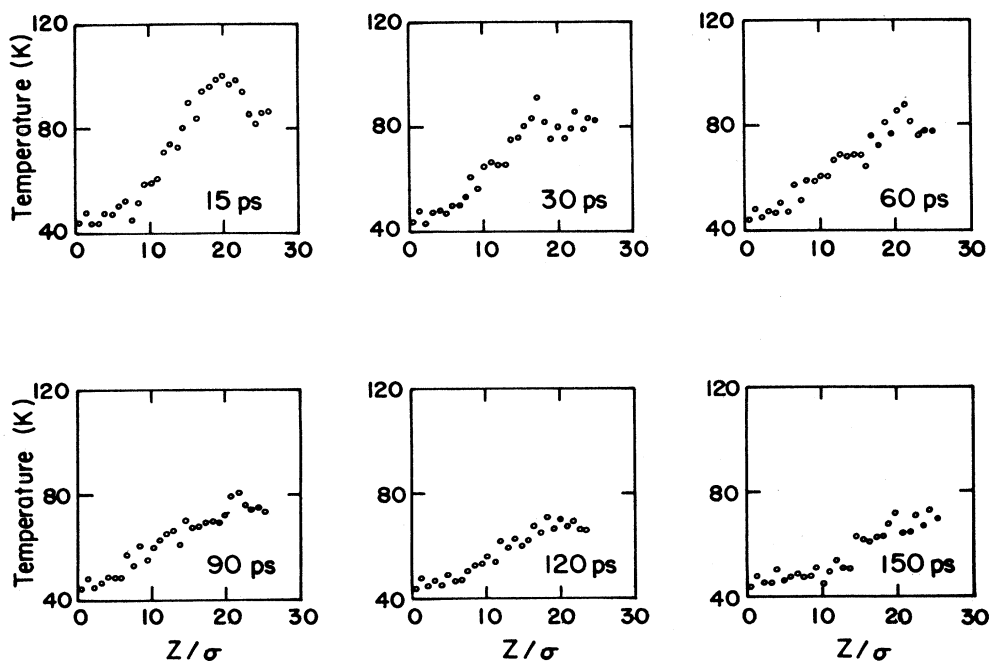
FIG. 4. Temperature profiles T/K as a function of position in the simulation cell, z/σ, at the same time intervals as Fig. 3. The mediation of the strong heat gradient as time increases is visible.
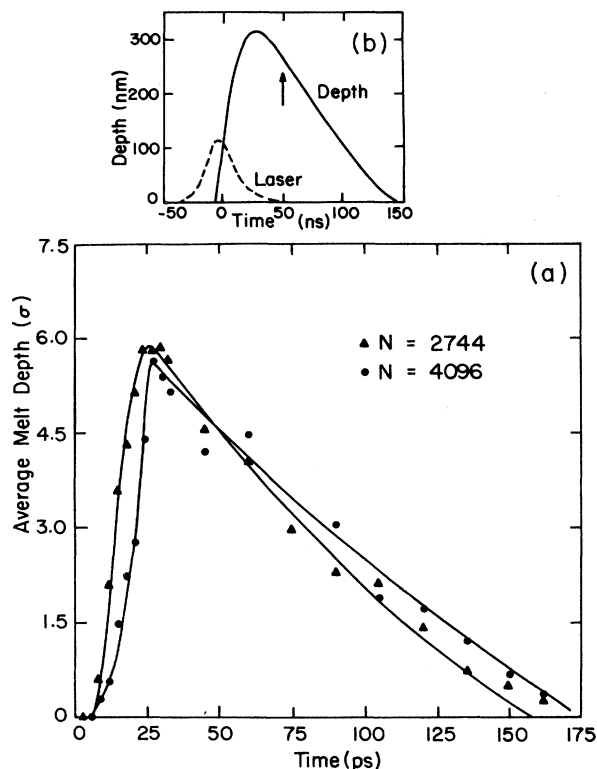
FIG. 5. (a) The average melt depth in units of σ as a function of time for two different system sizes, $N=2744$ ($\triangle$) and 4096 ($\bullet$). The solid lines represent polynomial fits to the simulation data. Inset above (b), for comparison, are experimental results for silicon (Ref. 36) following a 2-ns pulse.

FIG. 6. (a) The temperature of the interface, plotted as the difference from the melting temperature, as a function of time for two different system sizes, $N=2744$ ($\triangle$) and 4096 ($\bullet$). Inset above (b) are experimental results for silicon (Ref. 36). Key as in Fig. 5.

the important features found experimentally. There is a sharp rise in the melt depth during the rapid melt-in period and the melt continues to grow for about 5–8 ps after the "pulse" is "switched off." The melt depth reaches a maximum value followed by a period during which solidification occurs, caused by the rapid cooling. As the material cools, the melt thickness decreases, at a slower rate, until complete solidification takes place.

Given the instantaneous position of the solid-liquid interface, the temperature at the interface can be determined at any time from the temperature profiles (as in Fig. 4, for example). The simulation-produced interface temperature is shown as a function of time in Fig. 6, again shown with experimental interface temperatures for laser-annealed silicon.[36] There is considerable scatter in the simulation data. Nonetheless, a mean curve through these points again exhibits all the important characteristics of the experimental curve, as will be discussed in the next paragraph. The velocity of the interface is plotted as a function of time and of temperature in Figs. 7 and 8. By convention, the velocity during the melting phase is negative, whereas during the solidification phase it is positive. Figure 7 shows good qualitative agreement between these results and experiment[36] for the two very different substrates involved (LJ and silicon). The experimentally inaccessible "melt-in"

velocities can be seen to be determined from the simulation data.

A closer examination of the interface-temperature–versus–time (Fig. 6) and the interface-velocity–versus–time (Fig. 7) curves reveal the relationship between the heat flow, interface temperature, and the velocity of the interface. During the first 15 ps or so, when the rapid melting process occurs, the temperature at the interface rises rapidly and exceeds the equilibrium melting temperature (which for this system can be estimated from previous simulation results to be in the vicinity of $T^{*}=0.65$ or 78 K). The maximum interface temperature found in the simulation varies from 4 to 16 K above T_{m} (depending on N) and thus the extent of superheating is around 5–20 %. The velocity of the interface during this melt-in phase is very high, up to 90 m/s. Compared to this velocity, the rate at which atomic rearrangement takes place will be very slow. When the heating rate is very high compared to the kinetic time scale of atomic rearrangement, the solid will superheat.

At the end of the energy pulse, there is a sharp drop in temperature at the interface over a very short period of time due to the influence of conductivity to the substrate simulated via the heat bath. We have estimated a value for the temperature gradient close to the bottom of the cell from the temperature-position (T-z) profile. The
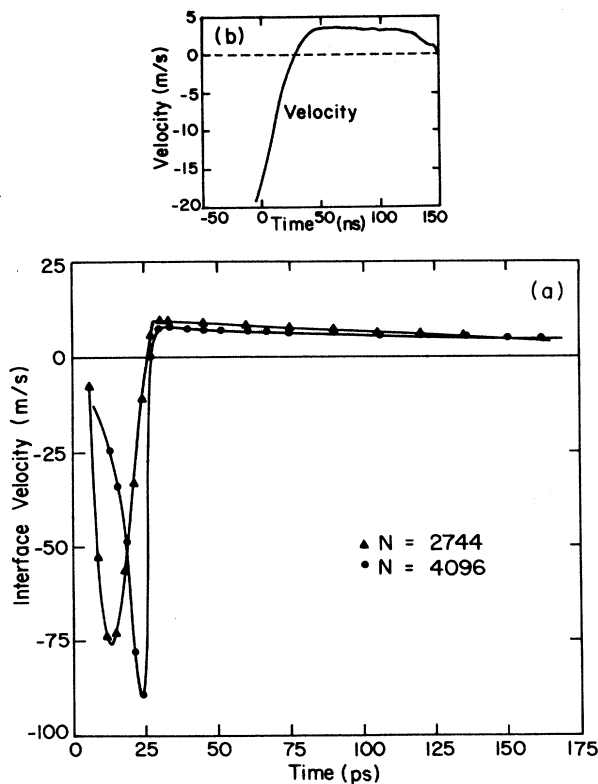
FIG. 7. (a) The interface velocity (in ms^{-1}) as a function of time for two different system sizes, $N=2744$ ($\triangle$) and 4096 ($\bullet$). Inset above (b) are experimental results for silicon (Ref. 36). Key as in Fig. 5.
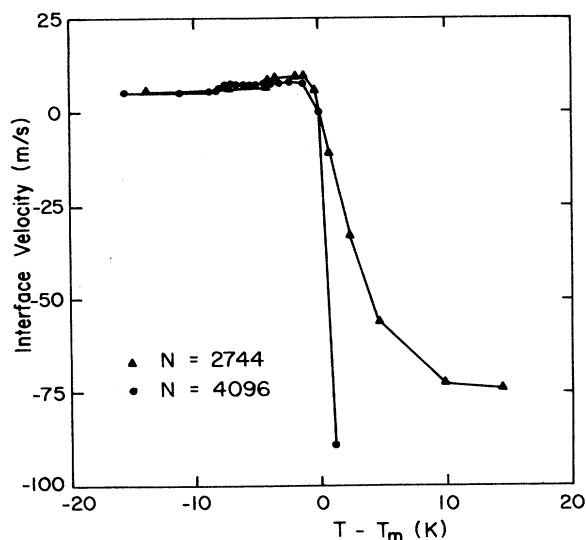
FIG. 8. The interface response function for Lennard-Jones atoms originally packed in a (100) fcc arrangement. The interface velocity (in ms^{-1}) is shown as a function of the temperature given as $T-T_m$ (in K). Key as in Fig. 5.

average value of this gradient during the steady-state growth regime is 7.3×10^9 K/m, comparing well with a value of 6.7×10^9 K/m which we have estimated from Landman's results.[24] The velocity scaling required in Landman's method is determined by the thermal conductivity (obtained from experimental data for argon) and the thermal gradient (obtained by a linear extrapolation to an imaginary point deep in the substrate), whereas in our method it was not fitted at all. All that should be construed from this is that the heat-conductivity–related properties for the Lennard-Jones atoms are about the same in both studies (as they should be), albeit achieved somewhat differently (Landman's by fitting to experimental data, ours being predicted).

Following the cessation of energy input, the melting process continues briefly and then solidification begins. The velocity of the interface decreases in magnitude as the temperature drops toward the equilibrium melting temperature T_m. When the temperature approaches T_m, the velocity of the interface goes to zero. This happens at around 27 ps. Once the "laser pulse" has been "switched off," the material cools very rapidly and the interface temperature drops below T_m. This undercooling now causes the solid-liquid interface to move in the direction of solidification, as evidenced by the growing positive velocity. Notwithstanding the scatter in the data, the extent of supercooling can be estimated roughly to be from 4 to 7.5 K below T_m (depending on N), i.e., around 5–10%.

Following this sharp drop in temperature, there is a long period (~ 70 ps) during which the undercooling persists at a more or less steady value. This constitutes a period of steady-state growth wherein the velocity of the interface remains at a steady value of 15 m/s (0.09 in reduced units) for $N=1000$. This value for the velocity of the interface agrees well with a reduced value of 0.10 obtained by Broughton et al.[21] for the steady-state velocity of the fcc (100) interface at $T^*=0.57$ (their system size being $N \sim 1500$). The larger systems predict a lower steady-state velocity of around 7.5–9.5 m/s. Eventually, heat conduction into the substrate cools the system and the interface temperature drops to the original temperature of the system. As solification approaches completion, the velocity tends to zero. The simulation has thus been shown to model successfully the properties and kinetics of the solid-liquid interface. Two further simulations were carried out with a small test system of $N=1000$ atoms subjected to 15-ps pulses of energy fluence, 43 and 60 mJ/cm^2, respectively. The melt-depth–versus–time curves for all three fluences are shown in Fig. 9. These curves exhibit the same qualitative features as the experimental data for silicon, at the same fluences, as measured by Bucksbaum and Bokor.[37] As expected, the melt front penetrates deeper into the solid for the higher fluences, the peaks occur at approximately the same times, and the system takes longer to anneal. One may also notice a long-time "tail" in all the depth curves shown in Fig. 9. This unwanted feature disappears for larger system sizes, as seen in Fig. 5.

The velocity-temperature relationship is shown in Fig. 8. The most striking feature of this curve is the apparent
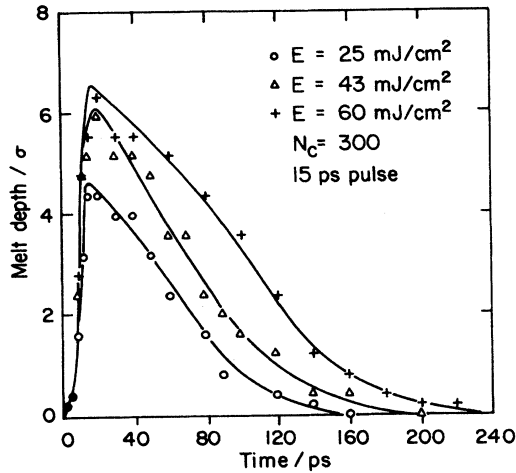
FIG. 9. Melt depth [as derived from an analysis of $g(r)$ data only] vs time for three simulations, in which $N = 1000$ LJ atoms were subjected to a 15-ps pulse with energy fluences 25 mJ/cm^2 (●), 43 mJ/cm^2 (△), and 60 mJ/cm^2 (+).

asymmetry between the melting and solidification region. Such an asymmetry has been suggested in recent experimental studies by Larson et al.[38] and by Tsao et al.[39] for silicon. However, experimental measurements have been unable, so far, to accurately determine the shape of the velocity-temperature curve, especially in the crucial region near $v = 0$. We calculated the slopes of the velocity-temperature curve in the region representing both solidification (positive v) and melting (negative v), with the results shown in Table I. This leads to a ratio of dV_m/dV_s of 3.1–11.8 (depending on N). It can be seen that the melting kinetics are considerably faster than the freezing kinetics for both system sizes, as predicted by the asymmetric theory. The reason for this asymmetry will be discussed in a forthcoming paper.[40] This work represents the first corroboration of the experimentally observed asymmetry by nonequilibrium computer simulation.

As a by-product of the simulation, it is also possible to assign a value to the equilibrium melting temperature as that at which the velocity is zero, at which point there is no driving force for the motion of the interface. This gives a value of $T_m^* = 0.65$–0.67 (depending on N) for our LJ system cut at $r_c^* = 3.0$. This result is in accord with earlier work which gives $T_m^* = 0.62$ for a LJ system cut at $r_c^* = 2.5$ (Ref. 19) and $T_m^* = 0.69$ for a full LJ potential ($r_c^* = \infty$) (Ref. 32, for example). It is perhaps worth noting that this is a very quick route to T_m compared to oth-

er simulation methods which typically involve numerous long simulation runs.[32] The only disadvantage is that the pressure is not held constant in this simulation; hence a certain amount of trial-and-error simulation would be necessary to achieve a desired value of the pressure; but it should still be a faster route to T_m.

A. Effect of the mass of an energy carrier

A systematic sensitivity analysis of the simulation method with respect to the variables in the simulation, partcularly m_c, N_c, and the size of the system, was undertaken in order to establish scale-up procedures and estimate the reproducibility of the results. In order to carry out the elastic collisions for the energy transfer, the energy carriers must have an associated mass. Its value is of no intrinsic interest except that changes in its value must not affect the simulations results to any significant extent. The results in the previous section showed that a mass ratio m_c/m of 10^{-6} gave satisfactory results, with nearly one-third of the solid melting. For $N = 1000$ and the same energy pulse as before, three runs were carried out with different values for m_c/m: 10^{-7}, 10^{-6}, and 10^{-5}.

With $m_c/m = 10^{-7}$, the mass of the energy carrier was found to be too small to have any influence on the solid. When m_c/m was increased to 10^{-5}, the mass of the energy carrier was sufficient to cause violent collisions with the substrate atoms, resulting in the complete destruction of the solid. These results indicate that there is only a narrow range of acceptable values of m_c/m. A value of the order of magnitude of 10^{-6} appears to be a satisfactory one, at least for a LJ system. It is not clear to what extent this is dependent on the intermolecular potential model; this will be determined in future studies as other materials are investigated.

B. Effect of the number of energy carriers

The number of energy carriers N_c determines the amount of material that will be affected by the energy-transfer process. The number of system atoms that undergo collisions with energy carriers at any instant of time is equal to the number of energy carriers minus the number of system atoms that are outside the "line of focus." As N_c is increased, a larger fraction of the initial solid is affected by the energy-transfer process, but this does not mean that a larger fraction of the solid melts. There is also an opposing effect, since the available energy per time step, ΔE, now has to be divided among more energy carriers and, subsequently, the energy transferred per collision is decreased. These two opposing effects give rise to an optimization situation. Since there is no

TABLE I. Melting and freezing asymmetry for LJ atoms.

System size N	Slope of solidification region dV_s/dT (m/K s)	Slope of melting region dV_m/dT (m/K s)	$(dV_m/dT)/(dV_s/dT)$
2744	−4.5858	−14.0671	3.0676
4096	−6.0413	−71.0397	11.7590

a priori relationship between N_c and the melt depth, simulations were carried out for different values of N_c in order to determine a unique value for N_c. This occurs at the maximum of the melt-depth–versus–N_c curve, as shown in Fig. 10.

For the same system and energy pulse used in Sec. IV, a series of simulations was carried out (with $N=1000$) with different values of N_c varying from 300 to 700. For a 1000-particle system, N_C cannot be increased above 700 since this would cause the energy carriers to interact with the heat bath. This defeats the purpose of the heat bath and jeopardizes the integrity of the simulation. From the melt-depth–versus–time curves, the maximum melt depth was determined for each case. These values of the maximum melt depth were plotted as a function of N_c, as shown in Fig. 10(a). This figure also shows the maximum fraction of initial solid melted versus N_c/N [Fig. 10(b)]. As N_c is increased, the maximum melt depth increases until a value for N_c (~ 600) is reached where it reaches a
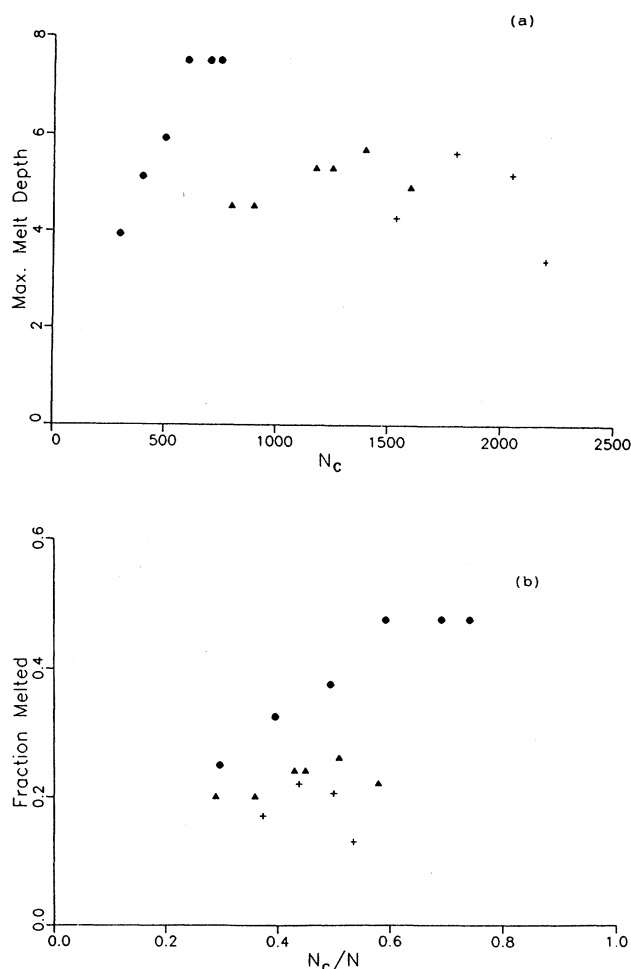
FIG. 10. (a) The maximum melt depth (in σ) as a function of the number of energy carriers, N_c. Results are shown for $N=1000$ (●), 2744 ($\triangle$), and 4096 (+). (b) The function of the substrate melted as a function of the fraction of the number of energy carriers to substrate atoms, N/N_c; key as in (a).

plateau value of 7.51σ, where the fraction of the original solid that has melted is 0.475. The value of N_c/N at which the plateau value is first reached is approximately 0.6, which means that approximately 60% of the system atoms have to undergo collisions in order to cause 47.5% of the solid to melt. The reason it is a plateau and not a maximum, as expected, is due to the poor statistics obtained with the small system size and to the effect of the heat bath for larger values of N_c. Under those circumstances, the cooling effect brought about by the heat bath, lying so close to the interface, creates a large temperature gradient. This gradient drives the interface deeper into the solid, although the collision process itself is not able to cause further melting. This, then, raises the issue of the system size to be used in these simulations, which will be discussed in the next section.

C. Effect of system size

The calculations in Sec. IV B were repeated for the two larger systems, $N=2744$ and 4096. For a pulse duration of 15 ps and $N=2744$, N_c was varied from 800 to 1600. The maximum melt-depth–versus–N plot and the fraction-melted–versus–(N_c/N) plot are shown in Fig. 10. In this case, a maximum can be seen at a N_c/N value of about 0.5. The maximum melt depth obtained in this case is about 5.70σ. For the $N=4096$ system, N_c was varied from 1536 to 2200. As shown in Fig. 10(a), the maximum melt depth is around 5.63σ where the value for N_c/N is about 0.45–0.47. From these results, it appears that a unique value for N_c is obtained when the number of energy carriers is approximately half the number of atoms in the system. The maximum melt depth of 7.51σ, obtained in the 1000-particle case, is probably an enhanced value due to the small size. The maximum melt depth for the two larger systems is approximately the same and this seems to suggest that a saturation value has been reached.

As shown in Figs. 5–9, there is essentially no difference between the results with $N=2744$ or 4096 for the resolidification portion of the diagrams. There is, however, some size dependence during the melt-in period. We have decided to proceed with the larger system in future studies, largely as insurance against the effect of the periodic boundary conditions. It was already noted that the $N=2744$ system shows less asymmetry in the interface response function. Studies of even larger systems are currently precluded given available computing resources.

D. Effect of changing the pulse duration

Calculations were carried out to test the sensitivity of melt-front penetration to the pulse-duration time. For a 1000-particle system, a 25-mJ/cm² energy pulse was used with a longer duration, 25 ps. The maximum melt depth obtained in this run was 5.85σ, as compared to 5.93σ obtained in Sec. IV C. These calculations showed that pulses of the same energy density but different duration will produce slightly different maximum melt depths, although the profiles are similar in shape. Though this difference is quite small and is within the error in the calculation, the trend is correct and is in agreement with the

results in Ref. 36. The melt-depth penetration is expected to decrease as the pulse duration is increased, chiefly because the same energy is now distributed over a larger interval of time, with the result that the energy available per time step is decreased. If the pulse duration is increased further, there will come a value for which no melting occurs at all.

V. DISCUSSION

A nonequilibrium molecular-dynamics–simulation technique has been developed to model the rapid melting and freezing processes that occur when a material is subjected to short (picosecond or nanosecond) pulses of energy. Although the method does not attempt to model the optical characteristics of the energy beam and the irradiated material, an energy-transfer mechanism has been developed by which the energy in the beam can be coupled with the material being processed. Using the LJ potential model as a test system, the ability of the method to successfully emulate the properties and kinetics of the transient solid-liquid interface was demonstrated. The interface temperature and interface velocity were calculated as functions of time and of each other and were shown to have all the characteristic features of experimentally determined results. The superheating and supercooling effects of the rapid heating and cooling caused by the pulsed energy input were demonstrated and related to the interface kinetics. The experimentally observed asymmetry in the interface response function was observed for the first time in a simulation study of laser annealing. Values predicted for the equilibrium melting temperature, steady-state solidification velocity, and heat gradient of the substrate compare well with other known results. Rules were developed for the determination of values for the simulation variables, the mass and number of energy carriers. It was determined that an appropriate value for m_c/m is of the order of 10^{-6} and that N_c/N should be 0.45–0.5. System-size effects were also investigated and it was found that both 2744- and 4096-particle systems gave very similar results for the resolidification process, but different results during the melt-in period. This resulted in less of an asymmetry between melting and freezing kinetics for the smaller-sized system. We suggest that this points to the (undesirable) influence of the periodic boundary conditions which, for the smaller system, would tend to facilitate recrystallization. Systems smaller than $N=2744$ are likely to produce qualitatively but not quantitatively, correct results. Now that the qualitative abilities of the method have been successfully demonstrated, we hope to complete experimental studies for the inert gases in order to assess the quantitative capabilities of the method, e.g., in terms of prediction

of the undercooling, and to establish relative time and length scales between experiment and theory. The model presented in this paper will then be refined as necessary.

Some comments regarding comparison with previous work are apropos at this point. We have established a nonequilibrium method for the transference of energy to the system, one relying on photon-emulating particles to exchange energy with the substrate via collisions rather than Landman's scaling of the velocities via a predetermined absorption profile. Our hope is that this will allow a more realistic method of energy transfer, since it involves molecular diffusional processes and less of an indirect influence on the resultant undercooling than is generated via an imposed profile. We also account in a simple way for reflectivity changes on melting, something which has not been done in previous NEMD studies. The properties presented in this paper were selected for their importance to those involved in directed thermal processing and are not to be found in any previous NEMD simulation paper. The method is also unique in that it was developed so that experimental values of the energy fluence could be used. It should also be noted that while an interface response function for the solidification of LJ atoms has been made for conditions representing a steady state in which the temperature was held constant,[21] our truly nonequilibrium method involves a substantial heat gradient, provides information about the melt-in process, predicts the extent of undercooling produced by the laser annealing conditions, and predicted a period of steady-state regrowth which evolved naturally in our simulation. The characteristics of this steady-state region agreed well with those in (Ref. 21). Thus much important information is available using nonequilibrium methods which is inaccessible by other steady-state methods.

The method of energy transfer also has the advantage over previous NEMD methods in that it can more readily be extended to the studies of other processes, such as ion implantation, and thus offers a flexible tool for the study of directed energy processing in general.

ACKNOWLEDGMENTS

*Author to whom correspondence should be addressed.

[1]B. C. Larson, C. W. White, T. S. Noogle, J. F. Barkost, and D. M. Mills, in *Laser-solid Interactions and Transient Thermal Processing of Materials*, edited by J. Narayan, W. L. Brown, and R. A. Lemons (North-Holland, New York, 1983), p. 43.

[2]S. U. Campisano, Appl. Phys. Lett. **45**, 398 (1984).

[3]C. G. Levi and R. Mehrabian, Metall. Trans. **11B**, 21 (1980).

[4]M. C. Flemings (unpublished).

[5]M. C. Fleming, in *Metallurgical Treatises* (American Society of Metallurgists, New York, 1981), p. 291.

[6]T. W. Clyne, Mater. Sci. Eng. **65-67**, 111 (1984).

[7]T. W. Clyne, Met. Technol. **11**, 350 (1984).

[8]P. Baeri, S. U. Campisano, G. Foti, and E. Rimini, J. Appl. Phys. **50**, 788 (1979).

[9]R. F. Wood and G. E . Giles, Phys. Rev. B **23**, 2923 (1981).

[10]R. F. Wood, J. R. Kirkpartick, and G. E. Giles, Phys. Rev. B **23**, 5555 (1981).

[11]R. F. Wood, Phys. Rev. B **25**, 2786 (1982).

[12]R. F. Wood and G. A. Geist, Phys. Rev. B **34**, 2606 (1986).

[13]J. N. Cape and L. V. Woodcock, Chem. Phys. Lett. **59**, 271 (1978).

[14]J. N. Cape and L. V. Woodcock, J. Chem. Phys. **73**, 2420 (1980).

[15]J. N. Cape, J. L. Finney, and L. V. Woodcock, J. Chem. Phys. **75**, 2366 (1981).

[16]A. J. C. Ladd and L. V. Woodcock, J. Phys. C **11**, 2565 (1978).

[17]J. Q. Broughton and L. V. Woodcock, J. Phys. C **11**, 2743 (1978).

[18]J. Q. Broughton and F. F. Abraham, Chem. Phys. Lett. **71**, 456 (1980).

[19]J. Q. Broughton, A. Bonissent, and F. F. Abraham, J. Chem. Phys. **74**, 4029 (1981).

[20]A. Bonissent and F. F. Abraham, J. Chem. Phys. **74**, 4029 (1981).

[21]J. Q. Broughton, G. H. Gilmer, and K. A. Jackson, Phys. Rev. Lett. **49**, 1496 (1982).

[22]J. Q. Broughton and G. H. Gilmer, J. Chem. Phys. **79**, 5095 (1983); **79**, 5105 (1983); **79**, 5119 (1983); **84**, 5741 (1986); **84**, 5749 (1986); **84**, 5759 (1986).

[23]F. F. Abraham and J. Q. Broughton, Phys. Rev. Lett. **56**, 734 (1986).

[24]U. Landman, C. L. Cleveland, and C. S. Brown, Phys. Rev. Lett. **45**, 2032 (1980).

[25]C. L. Cleveland, U. Landman, and R. N. Barnett, Phys. Rev. Lett. **49**, 790 (1982).

[26]U. Landman, R. N. Barnett, C. L. Cleveland, and R. H. Rast, J. Vac. Sci. Technol. A **3**, 1574 (1985).

[27]J. Q. Broughton and F. F. Abraham, J. Cryst. Growth **75**, 613 (1986).

[28]U. Landman, W. D. Leudtke, R. N. Barnett, C. L. Cleveland, M. W. Ribarsky, E. Arnold, S. Ramesh, H. Baumgart, A. Martinez, and B. Khan, Phys. Rev. Lett. **56**, 155 (1986); Vol. 53 of Materials Research Society Symposium Proceedings in *SOI-TFT Technology*, edited by A. Chiang, M. W. Geis, and L. Pfeiffer (MRS, Pittsburgh, 1986), p. 21.

[29]F. H. Stillinger and T. A. Weber, Phys. Rev. B **31**, 5262 (1985).

[30]M. D. Kluge, J. R. Ray, and A. Rahman, J. Chem. Phys. **87**, 2336 (1987).

[31]M. D. Kluge, J. R. Ray, and A. Rahman, Phys. Rev. B **36**, 4234 (1987).

[32]D. K. Chokappa and P. Clancy, Mol. Phys. **61**, 597, 616 (1987).

[33]D. Brown and J. H. R. Clarke, Mol. Phys. **51**, 1243 (1984).

[34]W. G. Hoover, Annu. Rev. Phys. Chem. **34**, 103 (1983).

[35]M. H. Grabow and G. H. Gilmer, Surf. Sci. **194**, 333 (1987).

[36]M. O. Thomspon, in *Energy-beam-solid Interactions and Transient Thermal Processing*, Vol. 35 of Materials Research Society Symposium Proceedings, edited by D. K. Biegelsen, G. A. Rozgonyi, and C. V. Shank (MRS, Pittsburgh, 1985), p. 181.

[37]P. H. Bucksbaum and J. Bokor, in *Laser-Solid Interactions and Transient Thermal Processing*, Vol. 13 of Materials Research Society Symposium Proceedings, edited by J. Narayan, W. L. Brown, and R. A. Lemons (MRS, Pittsburgh, 1983), p. 51.

[38]B. C. Larson, L. F. Tischler, and D. M. Mills, J. Mater. Res. **1**, 144 (1986).

[39]J. Y. Tsao, M. J. Aziz, M. O. Thompson, and P. S. Peercy, Phys. Rev. Lett. **56**, 2712 (1986).

[40]S. J. Cook and P. Clancy (unpublished).

[41]We use the interactive graphics program MOLPIC developed by Dr. S. M. Thompson, Cornell University.